Current-driven domain wall mobility in polycrystalline Permalloy nanowires: A numerical study

J. Leliaert, B. Van de Wiele, A. Vansteenkiste, L. Laurson, G. Durin, L. Dupré, and B. Van Waeyenberge

---

Articles you may be interested in

Current-driven domain wall motion in heterostructured ferromagnetic nanowires
Appl. Phys. Lett. **100**, 112401 (2012); 10.1063/1.3692797

Current-driven magnetic domain walls gather speed
Phys. Today **64**, 18 (2011); 10.1063/PT.3.1152

Direct imaging of current-driven domain walls in ferromagnetic nanostripes
J. Appl. Phys. **105**, 103902 (2009); 10.1063/1.3125526

Current-driven domain-wall depinning
J. Appl. Phys. **98**, 016108 (2005); 10.1063/1.1957122

Effect of Joule heating in current-driven domain wall motion
Appl. Phys. Lett. **86**, 012511 (2005); 10.1063/1.1847714

Current-driven domain wall mobility in polycrystalline Permalloy nanowires: A numerical study

J. Leliaert,[1,2,a)] B. Van de Wiele,[1] A. Vansteenkiste,[2] L. Laurson,[3] G. Durin,[4,5] L. Dupré,[1] and B. Van Waeyenberge[2]

[1]*Department of Electrical Energy, Systems and Automation, Ghent University, Sint-Pietersnieuwstraat 41, 9000 Gent, Belgium*
[2]*Department of Solid State Science, Ghent University, Krijgslaan 281/S1, 9000 Gent, Belgium*
[3]*COMP Centre of Excellence and Helsinki Institute of Physics, Department of Applied Physics, Aalto University School of Science, P.O. Box 11100, FI-00076 AALTO, Finland*
[4]*Istituto Nazionale di Ricerca Metrologica, Strada delle Cacce 91, 10135 Torino, Italy*
[5]*ISI Foundation, Via Alassio 11/c, 10126, Torino, Italy*

A complete understanding of domain wall motion in magnetic nanowires is required to enable future nanowire based spintronics devices to work reliably. The production process dictates that the samples are polycrystalline. In this contribution, we present a method to investigate the effects of material grains on domain wall motion using the GPU-based micromagnetic software package MuMax3. We use this method to study current-driven vortex domain wall motion in polycrystalline Permalloy nanowires and find that the influence of material grains is fourfold: an extrinsic pinning at low current densities, an increasing effective damping with disorder strength, shifts in the Walker breakdown current density, and the possibility of the vortex core to switch polarity at grain boundaries. © 2014 AIP Publishing LLC. [http://dx.doi.org/10.1063/1.4883297]

I. INTRODUCTION

A large number of future spintronics devices[1–3] are based on the controlled movement of domain walls through magnetic nanowires. To achieve this, a thorough understanding of domain wall mobility in real nanowires is of paramount importance. Research has mainly focused on domain wall motion in perfect nanowires[4,5] or nanowires with edge roughness.[6,7] However, it has recently been recognized that disorder distributed throughout the whole wire, as present in any real material, can have an important effect on the domain wall mobility.[8–10] Due to the imperfect fabrication process, distributed disorder exists on the atomistic scale (interstitials, vacancies, dislocations, etc.) and on the level of the material grains. Grain properties as grain size, thickness, etc., can vary, while the grain boundary corresponds with a misfit of the lattice structure of neighbouring grains. Numerical[10] and experimental[11–13] investigations show that distributed disorder gives rise to local pinning potentials. For a magnetic vortex in Permalloy, the potentials have a depth of 1 to 5 eV,[11,12,14] and an interaction range approximately equal to the vortex core diameter since the measured potential well is convolved with the vortex core profile.[11,13] Despite some controversy regarding the nature of the measured disorder,[14] a link with the grain structure of the material is suspected.[11,13] In this contribution, a method is presented to simulate polycrystalline materials in a computationally efficient way, and the influence on the current-driven mobility of vortex domain walls is investigated.

II. METHODS

We perform micromagnetic simulations using the GPU-based micromagnetic software package MuMax3,[15] which solves the Landau-Lifshitz equation[16] with spin-transfer-torque (STT) contributions[17]

$$\frac{\partial \mathbf{m}}{\partial t} = -\gamma_0 \mathbf{m} \times \mathbf{B}_{\text{eff}} + \alpha \mathbf{m} \times \frac{\partial \mathbf{m}}{\partial t} - [\mathbf{u} \cdot \nabla]\mathbf{m} + \beta \mathbf{m} \times [\mathbf{u} \cdot \nabla]\mathbf{m}. \quad (1)$$

Here, $\mathbf{m}$ is the space and time varying magnetization vector field, with a fixed amplitude $|\mathbf{m}| = 1$. Furthermore, γ_0 denotes the gyromagnetic ratio 1.7595×10^{11} rad/Ts and α is the dimensionless Gilbert damping constant. The effective field $\mathbf{B}_{\text{eff}}$ is the derivative with respect to $\mathbf{m}$ of the energy density ϵ with contributions of the exchange, anisotropy, Zeeman, and demagnetizing energy[18]

$$\mathbf{B}_{\text{eff}} = -\frac{1}{\gamma_0 M_s}\frac{\partial \epsilon}{\partial \mathbf{m}}. \quad (2)$$

The last two terms of equation (1) are the STT terms, taking into account the effects of a spin-polarized current running through the nanowire. The first STT-term represents the adiabatic interactions of the conduction electrons with the local magnetization, while the second term is a smaller non-adiabatic contribution with size β. Furthermore, $\mathbf{u}$ has the dimensions of a velocity

$$\mathbf{u} = \frac{g\mu_B P}{2eM_s}\mathbf{J}, \quad (3)$$

with g the Landé factor, μ_B the Bohr magneton, e the electron charge, and P the polarization of the current density $\mathbf{J}$.[19]

a)Electronic mail: jonathan.leliaert@ugent.be

In our simulations, we consider head-to-head magnetic domain walls. To efficiently simulate the domain wall motion in infinitely long magnetic nanowires, the computation is restricted to a window centered around the moving domain wall. To this end, the demagnetizing field introduced by the magnetic charges at the edges of the window is compensated by an opposite external field. The magnetization dynamics are evaluated by timestepping equation (1). Every timestep the simulation window is shifted to keep the domain wall centered, i.e., to keep the average magnetization component along the nanowire axis close to zero.

The grain structure of the polycrystalline material is implemented using a Voronoi tesselation, in which each Voronoi cell represents a grain. This approach enables one to define both edge roughness[6,20] and material grains.[21] Subdividing the material in grains starts with defining randomly distributed points (Voronoi centers) across the simulation geometry. A Voronoi cell consists of all points closest to a common Voronoi center. To cover the infinitely long simulation geometry, we virtually divide the nanowire into a grid of square tiles, sufficiently large so we can expect at least a few Voronoi centers per tile. Poisson statistics are used to determine the number of centers in the tile, while their positions are uniformly distributed over the tile using a random number generator with seed based on the tile index. This way we can map each discretization cell in the moving computational domain to a Voronoi cell without explicitly storing the complete tesselation along the wire. Indeed, when shifting the computational domain, new grains can be inserted from the sides based on the tile index. Also, as the simulation window might sometimes move backwards, this enables grains that previously left the simulation window to re-enter. Our implementation is sketched in Fig. 1, and an example is shown in Fig. 2.

Having subdivided the geometry, one can vary the local material parameters in and between the grains. This way, grain dependent anisotropy directions can represent the different lattice orientations in grains. However, Permalloy is specifically designed to minimize the influence of anisotropy on the magnetization dynamics. The other possibilities are grain dependent saturation magnetization representing thickness variations between grains[9] and reduced exchange stiffness at the grain boundaries representing a reduced magnetic coupling between neighbouring grains.[21] It is shown that both approaches to implement the influence of material grains on the magnetization dynamics can give rise to static pinning potentials corresponding to those that are experimentally found for distributed disorder.[10] In Sec. III, we investigate the influence of grains on the domain wall motion. To discriminate between the influence of thickness variations and reduced mutual exchange coupling, we treat them separately, while in real materials both effects are expected to play a role simultaneously.

We consider Permalloy nanowires of thickness 10 nm and width 400 nm discretized in finite difference cells of size $3.1255 \times 3.125 \times 10 \, \text{nm}^3$. The simulated time frame is 500 ns while the moving window around the domain wall is 1200 nm wide, and shifts with the domain wall. Material parameters typical for Permalloy are used: exchange stiffness
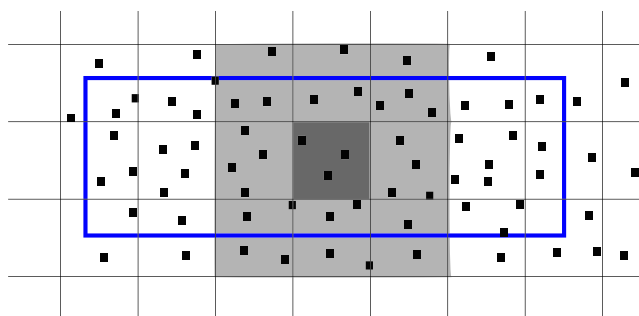

FIG. 1. The different Voronoi centers (black cells) are generated within the different tiles, with a random generator that uses the tile indices as a seed. For each discretization cell, the Voronoi cell to which it belongs is determined by looking for the closest Voronoi center in its own (dark grey) and all neighbouring (light grey) tiles. In this way also Voronoi centers outside the simulation window (blue) are found.

FIG. 2. An example of a nanowire with dimensions 200 nm × 1600 nm subdivided into Voronoi cells (grayscale) with average diameter 20 nm.

13×10^{-12} J/m, saturation magnetization 860×10^3 A/m, and Gilbert damping $\alpha = 0.01$ and 0.02. The average diameter of the Voronoi cells is 10 nm, which corresponds to the thickness of the nanowire. First, the influence of the grain boundaries is studied by reducing the exchange stiffness from 100% to 30% of the original value in steps of 10%. Second, the influence of grain thickness fluctuations is studied by varying the saturation magnetization within the different grains. A maximum deviation Δ of the average saturation magnetization M_s is considered from 0% to 25% in steps of 5%. In a given simulation, the saturation magnetization for each grain is taken randomly from the set $\{M_s - \Delta, M_s - \Delta/2, M_s, M_s + \Delta/2, M_s + \Delta\}$.

The domain wall motion is driven by spin-polarized currents. While some experiments based on domain wall motion[22–25] report values for the degree of non-adiabaticity $\beta \approx \alpha$, it was recently shown[38] that the scheme used to extract β is compromised by the effects of disorder. Therefore, we follow experiments suggesting that $\beta > \alpha$ for Permalloy[26–33] and use $\beta = 2\alpha$.

The depth of the pinning potentials caused by disorder[10] is an order of magnitude larger than an energy $k_B T$ at T = 300 K (k_B is the Boltzmann constant). Therefore, thermal effects on the domain wall mobility are negligible and the nanowires are simulated at a temperature of 0 K.

III. RESULTS AND DISCUSSION

A. Non-disordered nanowires

To understand the influence of material grains on domain wall motion, we first consider the dynamics in a nanowire without disorder. The considered cross-sectional dimensions of the nanowire dictate that the static equilibrium domain wall configuration is a vortex wall.[34] A vortex wall
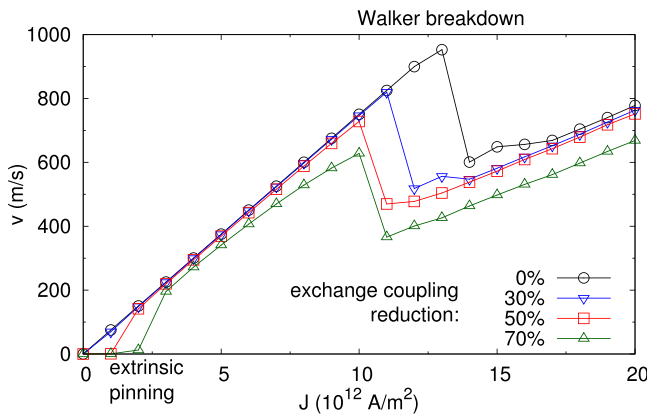
FIG. 3. Velocity vs. applied current density of vortex domain walls in poly-crystalline nanowires with different reductions of the exchange stiffness at the grain boundaries. For increasing exchange reductions, a larger extrinsic pinning takes place, the slope of the mobility curve is reduced, and the Walker breakdown is shifted towards lower current densities.

FIG. 5. Velocity vs. applied current density of vortex domain walls in poly-crystalline nanowires with different variations in the saturation magnetization. For larger reductions, an extrinsic pinning takes place and the slope of the mobility curve lowers.

(Fig. 4) is a domain wall in which the magnetization rotates around a vortex core with out-of-plane magnetization. Figure 3 shows that for a non-disordered wire, i.e., without reduction in exchange coupling or thickness variations, two linear velocity vs. applied current regimes are separated by the Walker breakdown (WB). Below the Walker breakdown, the vortex domain wall transforms into a transverse domain wall that moves along the wire without changing its shape, resulting in a constant velocity which is linearly dependent on the

applied current (Fig. 4). Above the Walker breakdown, the transverse wall is no longer stable and a periodic motion with successive transformations from vortex to transverse domain wall structure and vice versa takes place. Since vortex walls move at lower velocity than transverse domain walls for the same applied current, this results in a sudden drop in domain wall velocity at the Walker breakdown. Above the Walker breakdown, the velocity increases again with growing current densities (Fig. 3).

B. Polycrystalline nanowires

We initialize the magnetization as a transverse domain wall, as this is the only stable state in non-disordered nanowires below the Walker breakdown at non-zero current densities. The mobility of this domain wall is simulated with different reductions in exchange coupling between the grains, as shown in Fig. 3. Figure 5 shows similar mobility curves for grains simulated as variations in the saturation magnetization. Both Figs. 3 and 5 show that at low current densities, the disorder is able to pin the magnetic domain wall. This extrinsic pinning mechanism[8] gets stronger for larger reductions in the exchange coupling and larger variations in saturation magnetization as the depth of the corresponding pinning potential increases.[10]

Below the Walker breakdown and above the depinning threshold, the velocity v depends linearly on the current density J. From the analytical one-dimensional model,[35] it is known that the slope of this curve is proportional to β/α. Disorder in the nanowires makes the medium through which the domain wall moves more viscous, giving rise to a larger effective damping parameter[8] $\alpha_{eff} = \alpha_{int} + \alpha_{ext}$. α_{int} is the Gilbert damping constant that dictates how fast energy is irreversibly dissipated to the lattice while α_{ext} arises from energy transfer to other modes by the scattering processes within the magnetic system,[36] for example, the emission of spin waves. To determine α_{ext}, we fit β/α_{eff} to the slope of the mobility curves as a function of the reduction in the exchange coupling or the variation in the saturation magnetization for $\alpha_{int} = 0.01$ and $\alpha_{int} = 0.02$. Fig. 6 shows in both cases a similar increase in α_{ext} for a growing average pinning
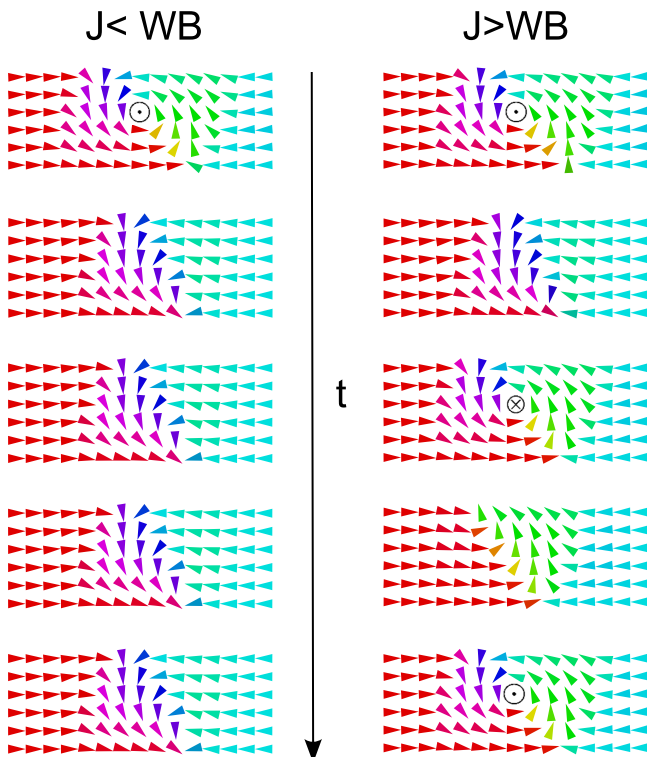

FIG. 4. Vortex domain wall motion in a non-disordered nanowire. Below the WB, the vortex wall transforms into a transverse wall with fixed shape although this is not the equilibrium state in the absence of an applied current. Above the Walker breakdown, the vortex wall periodically transforms between vortex and transverse walls.
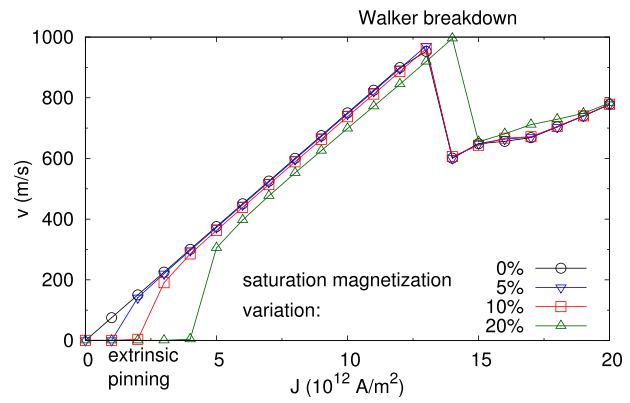
FIG. 6. α_{ext} as function of the disorder strength for two different implementations of grains: a reduction in exchange coupling at the grain boundaries or a variation in the saturation magnetization between different grains. α_{ext} was calculated from mobility curves for $\alpha_{int} = 0.01$(red crosses) and $\alpha_{int} = 0.02$ (blue circles).
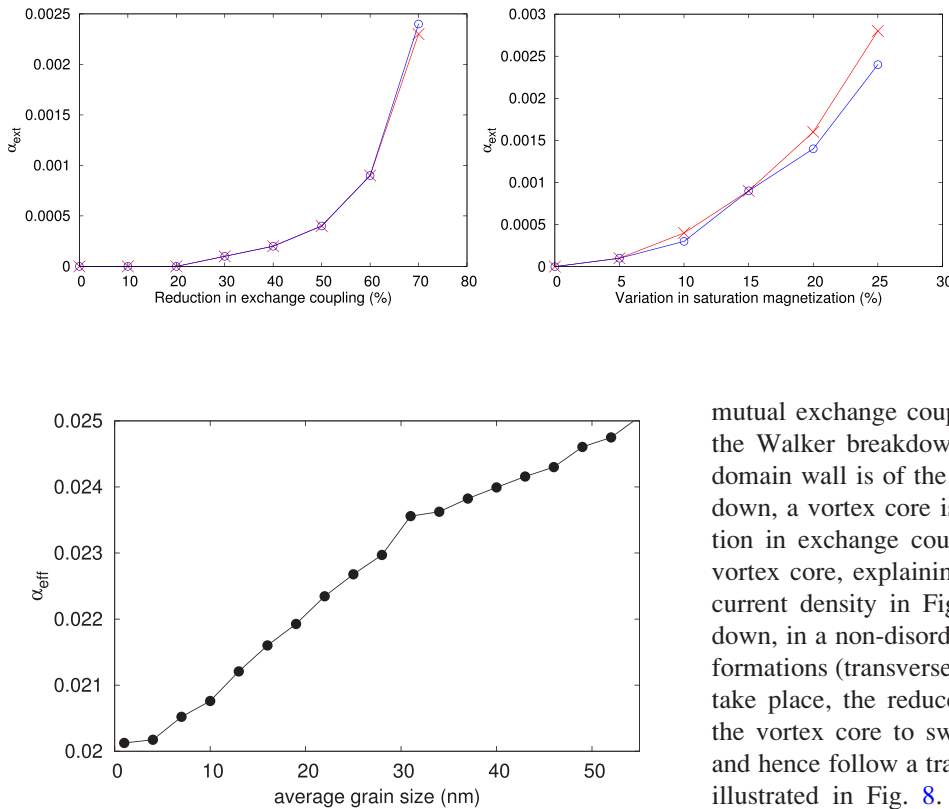

FIG. 7. Effective damping (α_{eff}) for different average grain sizes. All values were determined for $\alpha_{int} = 0.02$ and $\Delta M_s = 15\%$.

strength of the grains. This observation justifies the splitup of α_{eff} into a constant intrinsic part, and an extrinsic part depending on the disorder in the magnetic system. The relative effect of disorder becomes increasingly important in systems with a small intrinsic damping. To further investigate the extrinsic damping, we vary the average grain diameter and determine α_{eff}. The results are shown in Fig. 7. We see that α_{eff} and thus α_{ext} increase for larger grain diameters, which is in correspondence with experimental results.[37] This is explained as follows. Every grain gives rise to a potential well which contains a discrete spectrum of energy levels. When the domain wall enters a grain, it excites spin waves. When the wavelength of these spin waves corresponds to one of the energy levels, the spin wave remains in the potential well of the grain and damps out. In larger grains, more energy levels get excited and the resulting damping is larger.

In Ref. 10, it was shown that a single defect simulated as either a region with reduced saturation magnetization or exchange coupling can give rise to equivalent potential wells. However, depending on the simulation approach, the collective influence of the ensemble of grains on the domain wall dynamics differs: only grains simulated with a reduced

mutual exchange coupling have a large effect at and above the Walker breakdown. Below the Walker breakdown, the domain wall is of the transverse type. At the Walker breakdown, a vortex core is nucleated at the wire edge. A reduction in exchange coupling facilitates the nucleation of the vortex core, explaining the reduction in Walker breakdown current density in Fig. 3. While above the Walker breakdown, in a non-disordered wire, periodic domain wall transformations (transverse to vortex domain wall and vice versa) take place, the reduced mutual exchange coupling enables the vortex core to switch polarization at a grain boundary and hence follow a trajectory near the middle of the wire, as illustrated in Fig. 8. Here, the vortex domain wall never transforms into the transverse domain wall explaining the reduced domain wall velocity above the Walker breakdown. This motion resembles the motion of a vortex wall in a non-disordered wire for $\beta = \alpha$, which is elaborated in more detail in Ref. 38. Both phenomena originate from the large effect of local exchange stiffness variations on the vortex core stability. On the contrary, the effect on the core stability of variations in the saturation magnetization is much weaker. Consequently, the effect on the Walker breakdown current density is negligible and we do not observe vortex core switching. Hence, also the domain wall velocity above the Walker breakdown is hardly affected (Fig. 5).

IV. CONCLUSION

In conclusion, we have presented a computationally efficient method to simulate polycrystalline nanowires and have employed it to investigate the influence of material grains on current driven domain wall motion. We discriminate between the influence of thickness variations and reduced mutual coupling between grains and find that the influence of grains on the domain wall dynamics is fourfold. First, an extrinsic pinning regime at low current densities appears. Second, under the Walker breakdown, an effective damping parameter α_{eff} lowers the slope of the mobility curves. This damping parameter consists of a constant intrinsic part and

FIG. 8. The trajectory of a vortex wall moving through a polycrystalline Permalloy nanowire, 400 nm wide and 10 nm thick. The core is driven by a current density of 17×10^{12} A/m^2 which is larger than the Walker breakdown. The exchange coupling at the grain boundaries is reduced to 40% of its original value. The white/black colors indicate a positive/negative vortex core polarization. The core switches its polarization at a grain boundary and consequently changes its transverse propagation direction. As a result, the vortex core stays in the body of the nanowire and the domain wall never transforms into a transverse wall.
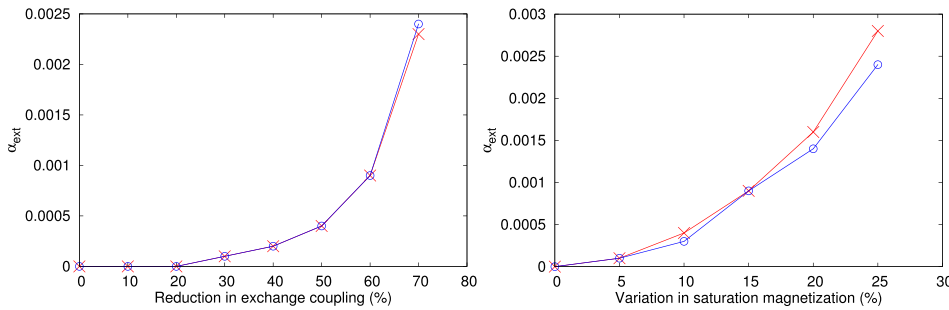
an extrinsic part which depends on the disorder strength. Third, only the reduced exchange coupling between grains facilitates the nucleation of a vortex core, resulting in a lower Walker breakdown current density and, fourth, the vortex core is able to switch its polarization at a grain boundary. Therefore, above the Walker breakdown, the vortex domain wall does not transform into a transverse domain wall and the vortex core continues to move in the body of the nanowire. This work complements earlier studies with edge roughness, which also has an influence on the mobility of the domain walls.[6]

We presented specific case studies of current driven domain wall motion in Permalloy nanowires. However, the code is freely available[15] and can be used to investigate the influence of material grains in other micromagnetic systems. In further research, it could be applied to the influence of grains on domain wall motion in perpendicular magnetic anisotropy (PMA) materials[39] where very large damping is measured ($\alpha_{eff} = 0.15$ in Ref. [40]). This might be due to an extrinsic damping originating in the polycrystalline structure of the samples.

[1]D. A. Allwood, G. Xiong, C. C. Faulkner, D. Atkinson, D. Petit, and R. P. Cowburn, "Magnetic domain-wall logic," Science **309**(5741), 1688–1692 (2005).

[2]S. E. Barnes, J. Ieda, and S. Maekawa, "Magnetic memory and current amplification devices using moving domain walls," Appl. Phys. Lett. **89**(12), 122507 (2006).

[3]S. P. Parkin, M. Hayashi, and L. Thomas, "Magnetic domain-wall racetrack memory," Science **320**(5873), 190–194 (2008).

[4]A. Thiaville and Y. Nakatani, *Spin Dynamics in Confined Magnetic Structures III*, Topics in Applied Physics Vol. 101/2006 (Springer, Berlin–Heidelberg, 2006), Chap. Domain-wall dynamics in nanowires and nanostrips, pp. 161–205.

[5]O. Boulle, G. Malinowski, and M. Kläui, "Current-induced domain wall motion in nanoscale ferromagnetic elements," Mater. Sci. Eng., R **72**(9), 159–187 (2011).

[6]Y. Nakatani, A. Thiaville, and J. Miltat, "Faster magnetic walls in rough wires," Nature Mater. **2**, 521–523 (2003).

[7]E. Martinez, "Micromagnetic analysis of current-driven dw dynamics along rough strips with high perpendicular anisotropy at room temperature," J. Magn. Magn. Mater. **324**(21), 3542–3547 (2012).

[8]B. V. de Wiele, L. Laurson, and G. Durin, "Effect of disorder on transverse domain wall dynamics in magnetic nanostrips," Phys. Rev. B **86**, 144415 (2012).

[9]H. Min, R. D. McMichael, M. J. Donahue, J. Miltat, and M. D. Stiles, "Effects of disorder and internal dynamics on vortex wall propagation," Phys. Rev. Lett. **104**, 217201 (2010).

[10]J. Leliaert, B. Van de Wiele, A. Vansteenkiste, L. Laurson, G. Durin, L. Dupré, and B. Van Waeyenberge, "A numerical approach to incorporate intrinsic material defects in micromagnetic simulations," J. Appl. Phys. **115**(17), 17D102 (2014).

[11]T. Y. Chen, M. J. Erickson, P. A. Crowell, and C. Leighton, "Surface roughness dominated pinning mechanism of magnetic vortices in soft ferromagnetic films," Phys. Rev. Lett. **109**, 097202 (2012).

[12]J. A. J. Burgess, A. E. Fraser, F. Fani Sani, D. Vick, B. D. Hauer, J. P. Davis, and M. R. Freeman, "Quantitative magneto-mechanical detection and control of the barkhausen effect," Science **339**(6123), 1051–1054 (2013).

[13]R. L. Compton, T. Y. Chen, and P. A. Crowell, "Magnetic vortex dynamics in the presence of pinning," Phys. Rev. B **81**, 144412 (2010).

[14]J.-S. Kim, O. Boulle, S. Verstoep, L. Heyne, J. Rhensius, M. Kläui, L. J. Heyderman, F. Kronast, R. Mattheis, C. Ulysse, and G. Faini, "Current-induced vortex dynamics and pinning potentials probed by homodyne detection," Phys. Rev. B **82**(10), 104427 (2010).

[15]A. Vansteenkiste and B. Van de Wiele, "Mumax: A new high-performance micromagnetic simulation tool," J. Magn. Magn. Mater. **323**(21), 2585–2591 (2011).

[16]L. D. Landau and E. M. Lifshitz, "Theory of the dispersion of magnetic permeability in ferromagnetic bodies," Phys. Z. Sowietunion **8**, 153 (1935).

[17]S. Zhang and Z. Li, "Roles of nonequilibrium conduction electrons on the magnetization dynamics of ferromagnets," Phys. Rev. Lett. **93**(12), 127204 (2004).

[18]L. Lopez-Diaz, D. Aurelio, L. Torres, E. Martinez, M. A. Hernandez-Lopez, J. Gomez, O. Alejos, M. Carpentieri, G. Finocchio, and G. Consolo, "Micromagnetic simulations using graphics processing units," J. Phys. D: Appl. Phys. **45**(32), 323001 (2012).

[19]G. S. D. Beach, M. Tsoi, and J. L. Erskine, "Current-induced domain wall motion," J. Magn. Magn. Mater. **320**(7), 1272–1281 (2008).

[20]H. Tanigawa, T. Koyama, M. Bartkowiak, S. Kasai, K. Kobayashi, T. Ono, and Y. Nakatani, "Dynamical pinning of a domain wall in a magnetic nanowire induced by walker breakdown," Phys. Rev. Lett. **101**(20), 207203 (2008).

[21]J. W. Lau, R. D. McMichael, and M. J. Donahue, "Implementation of two-dimensional polycrystalline grains in object oriented micromagnetic framework," J. Res. Natl. Inst. Stand. Technol. **114**(1), 57 (2009).

[22]G. Meier, M. Bolte, R. Eiselt, B. Krüger, D.-H. Kim, and P. Fischer, "Direct imaging of stochastic domain-wall motion driven by nanosecond current pulses," Phys. Rev. Lett. **98**(18), 187202 (2007).

[23]M. Hayashi, L. Thomas, Ya. B. Bazaliy, C. Rettner, R. Moriya, X. Jiang, and S. S. P. Parkin, "Influence of current on field-driven domain wall motion in permalloy nanowires from time resolved measurements of anisotropic magnetoresistance," Phys. Rev. Lett. **96**(19), 197207 (2006).

[24]G. S. D. Beach, C. Knutson, C. Nistor, M. Tsoi, and J. L. Erskine, "Nonlinear domain-wall velocity enhancement by spin-polarized electric current," Phys. Rev. Lett. **97**(5), 057203 (2006).

[25]L. Heyne, J. Rhensius, A. Bisig, S. Krzyk, P. Punke, M. Kläui, L. J. Heyderman, L. Le Guyader, and F. Nolting, "Direct observation of high velocity current induced domain wall motion," Appl. Phys. Lett. **96**(3), 032504 (2010).

[26]S. Lepadatu, A. Vanhaverbeke, D. Atkinson, R. Allenspach, and C. H. Marrows, "Dependence of domain-wall depinning threshold current on pinning profile," Phys. Rev. Lett. **102**(12), 127203 (2009).

[27]S. Lepadatu, M. C. Hickey, A. Potenza, H. Marchetto, T. R. Charlton, S. Langridge, S. S. Dhesi, and C. H. Marrows, "Experimental determination of spin-transfer torque nonadiabaticity parameter and spin polarization in permalloy," Phys. Rev. B **79**(9), 094402 (2009).

[28]S. Lepadatu, J. S. Claydon, C. J. Kinane, T. R. Charlton, S. Langridge, A. Potenza, S. S. Dhesi, P. S. Keatley, R. J. Hicken, B. J. Hickey, and C. H. Marrows, "Domain-wall pinning, nonadiabatic spin-transfer torque, and spin-current polarization in permalloy wires doped with vanadium," Phys. Rev. B **81**(2), 020413 (2010).

[29]M. Eltschka, M. Wötzel, J. Rhensius, S. Krzyk, U. Nowak, M. Kläui, T. Kasama, R. E. Dunin-Borkowski, L. J. Heyderman, H. J. van Driel, and R. A. Duine, "Nonadiabatic spin torque investigated using thermally activated magnetic domain wall dynamics," Phys. Rev. Lett. **105**(5), 056601 (2010).

[30]L. Thomas, M. Hayashi, X. Jiang, R. Moriya, C. Rettner, and S. S. P. Parkin, "Oscillatory dependence of current-driven magnetic domain wall motion on current pulse length," Nature **443**(7108), 197–200 (2006).

[31]L. Heyne, J. Rhensius, D. Ilgaz, A. Bisig, U. Rüdiger, M. Kläui, L. Joly, F. Nolting, L. J. Heyderman, J. U. Thiele, and F. Kronast, "Direct determination of large spin-torque nonadiabaticity in vortex core dynamics," Phys. Rev. Lett. **105**(18), 187203 (2010).

[32]S. D. Pollard, L. Huang, K. S. Buchanan, D. A. Arena, and Y. Zhu, "Direct dynamic imaging of non-adiabatic spin torque effects," Nat. Commun. **3**, 1028 (2012).

[33]J.-Y. Chauleau, H. G. Bauer, H. S. Körner, J. Stigloher, M. Härtinger, G. Woltersdorf, and C. H. Back, "Self-consistent determination of the key spin-transfer torque parameters from spin-wave doppler experiments," Phys. Rev. B **89**, 020403 (2014).

[34]Y. Nakatani, A. Thiaville, and J. Miltat, "Head-to-head domain walls in soft nano-strips: A refined phase diagram," J. Magn. Magn. Mater. **290–291**, 750–753 (2005).

[35]A. Thiaville, Y. Nakatani, J. Miltat, and Y. Suzuki, "Micromagnetic understanding of current-driven domain wall motion in patterned nanowires," Europhys. Lett. **69**, 990–996 (2005).

[36]K. Lenz, H. Wende, W. Kuch, K. Baberschke, K. Nagy, and A. Jánossy, "Two-magnon scattering and viscous gilbert damping in ultrathin ferromagnets," Phys. Rev. B **73**, 144424 (2006).

[37]J. Rantschler, Y. Ding, S.-C. Byeon, and C. Alexander, Jr., "Microstructure and damping in FeTiN and CoFe films," J. Appl. Phys. **93**(10), 6671–6673 (2003).

[38]J. Leliaert, B. V. de Wiele, A. Vansteenkiste, L. Laurson, G. Durin, L. Dupré, and B. V. Waeyenberge, "Influence of material defects on current-driven vortex domain wall mobility," Phys. Rev. B **89**, 064419 (2014).

[39]E. Martinez, "Static properties and current-driven dynamics of domain walls in perpendicular magnetocrystalline anisotropy nanostrips with rectangular cross-section," *Adv. Condens. Matter Phys.* 2012, 954196.

[40]O. Boulle, J. Kimling, P. Warnicke, M. Kläui, U. Rüdiger, G. Malinowski, H. J. M. Swagten, B. Koopmans, C. Ulysse, and G. Faini, "Nonadiabatic spin transfer torque in high anisotropy magnetic nanowires with narrow domain walls," Phys. Rev. Lett. **101**, 216601 (2008).